



HHS Public Access

Author manuscript

J Neurochem. Author manuscript; available in PMC 2021 April 01.

Published in final edited form as:

J Neurochem. 2020 April ; 153(2): 203–215. doi:10.1111/jnc.14971.

ASIC1a Channels Regulate Mitochondrial Ion Signaling and Energy Homeostasis in Neurons

Ivana Savic Azoulay^{1,*}, Fan Liu^{2,*}, Qin Hu², Maya Rozenfeld¹, Tsipi Ben Kasus Nissim¹, Michael X Zhu³, Israel Sekler¹, Tian-Le Xu²

¹Department of Physiology and Cell Biology, Faculty of Health Sciences, Ben-Gurion University of the Negev, Beer-Sheva, 84105, Israel

²Collaborative Innovation Center for Brain Science, Department of Anatomy and Physiology, Shanghai Jiao Tong University School of Medicine, Shanghai 200025, China

³Department of Integrative Biology and Pharmacology, McGovern Medical School, The University of Texas Health Science Center at Houston, Houston 77030, USA

Abstract

Acid sensing ion channel 1a (ASIC1a) is well-known to play a major pathophysiological role during brain ischemia linked to acute acidosis of ~ pH 6, while its function during physiological brain activity, linked to much milder pH changes, is still poorly understood. Here, by performing live cell imaging utilizing Na⁺ and Ca²⁺ sensitive and spatially specific fluorescent dyes, we investigated the role of ASIC1a in cytosolic Na⁺ and Ca²⁺ signals elicited by a mild extracellular drop from pH 7.4 to 7.0 and how these affect mitochondrial Na⁺ and Ca²⁺ signaling or metabolic activity. We show that in mouse primary cortical neurons, this small extracellular pH change triggers cytosolic Na⁺ and Ca²⁺ waves that propagate to mitochondria. Inhibiting ASIC1a with Psalmotoxin 1 (PcTX1) or ASIC1a gene knockout blocked not only the cytosolic but also the mitochondrial Na⁺ and Ca²⁺ signals. Moreover, physiological activation of ASIC1a by this pH shift enhances mitochondrial respiration and evokes mitochondrial Na⁺ signaling even in digitonin - permeabilized neurons. Altogether our results indicate that ASIC1a is critical in linking physiological extracellular pH stimuli to mitochondrial ion signaling and metabolic activity and thus is an important metabolic sensor.

Graphical Abstract

Acid sensing ion channel 1a (ASIC1a) plays a major pathophysiological role during brain ischemia linked to acute acidosis of ~ pH 6. We show that a milder physiologically relevant

Correspondence should be addressed to: T.L.X (xu-happiness@shsmu.edu.cn), M.X.Z (Michael.X.Zhu@uth.tmc.edu) and I.S. (sekler@bgu.ac.il).

*These authors contributed equally to this work

Author contribution

Ivana Savic Azoulay, Israel Sekler, Michael X Zhu, wrote the manuscript; Fan Liu, Tsipi Ben Kasus Nissim and Tian-Le Xu wrote the text and designed the experiments of the revised manuscript; Ivana Savic Azoulay, Fan Liu and Maya Rozenfeld performed the experiments; Michael X Zhu, Israel Sekler and Tian-Le Xu provided experimental oversight; Ivana Savic Azoulay, Fan Liu, Israel Sekler, Qin Hu, Michael X Zhu and Tian-Le Xu designed the experiments; Ivana Savic Azoulay, Fan Liu, Qin Hu, Israel Sekler, Michael X Zhu, and Tian-Le Xu interpreted the data.

Conflict of interest

Authors declared no conflict of interest

extracellular pH change from 7.4 to 7.0 triggers ASIC1a a -dependent cytosolic Na⁺ and Ca²⁺ signals that propagate to mitochondria. Activation of ASIC1a by this 7.4-7.0 pH shift also increases mitochondrial metabolism and respiration. Our results indicate that ASIC1a dependent Na⁺ and Ca²⁺ signaling links physiological extracellular pH shift to mitochondrial ion signaling and metabolic activity by invoking ionic signals that propagate from cytosol to mitochondria.

Keywords

ASIC1a; cytosolic Na⁺ signaling; cytosolic Ca²⁺ signaling; mitochondrial Na⁺ signaling; mitochondrial Ca²⁺ signaling; NCLX

Introduction

Acid sensing ion channels (ASICs) are proton-gated sodium-selective channels localized in the central and peripheral nervous systems (Krishtal 2003, Wu, Duan et al. 2004) and other types of tissues (Jahr, van Driel et al. 2005, Grifoni, Jernigan et al. 2008). So far, 6 subtypes of ASICs have been described, with ASIC1a being the major subtype expressed in neurons of the central nervous system (Waldmann, Champigny et al. 1997). In addition to conducting Na⁺, ASIC1a also exhibits Ca²⁺ permeability (Grunder and Chen 2010, Grunder and Pusch 2015, Waldmann, Champigny et al. 1997). Binding of H⁺ to an extracellular domain of ASIC1a causes channel pore opening and Na⁺ (Ca²⁺) influx into the cell (Krishtal 2003).

The functional significance of ASIC1a has been primarily associated with synaptic plasticity (Chiang, Chien et al. 2015, Liu, Yan et al. 2016, Tian, Wang et al. 2016) and acid-induced neuronal cell death under pathophysiological conditions such as those that occur in brain ischemia or other brain insults when extracellular pH drops to pH 6.0 or below (Wemmie, Chen et al. 2002, Askwith, Wemmie et al. 2004). However, learning impairments of ASIC1a knockout (KO) mice (Coryell, Wunsch et al. 2008) suggest that this channel has an important, but poorly understood, physiological function (Wemmie, Chen et al. 2002). While severe tissue acidosis leading to a ~ pH 6 drop is linked to brain ischemia, a much milder acidification triggered, for example, by astrocytic lactate production is a hallmark of regular metabolic processes (Pellerin, Pellegrini et al. 1998). How such moderate acidification affects ASIC1a and if ASIC1a -transmitted -pH dependent -signal is transferred to the metabolic hub of the cell- mitochondria still remain elusive.

Mitochondria play a critical role in cellular energy production and Ca²⁺ shuttling which is linked to several aspects of metabolic and global Ca²⁺ regulation. At least 3 enzymes of Krebs' cycle are activated by an intra-mitochondrial Ca²⁺ rise (McCormack and Denton 1990), linking Ca²⁺ signaling to ATP production (Griffiths and Rutter 2009). Acidification of extracellular and intracellular environment affects cell and mitochondrial metabolism by changing Ca²⁺ signaling properties and ATP production (Zima, Pabbidi et al. 2013), but whether ASIC1a participates in this process remains unknown. Here we asked if extracellular acidification can affect mitochondrial function by transmitting Na⁺ and Ca²⁺ transients and thereby controlling their metabolic activity. In this context, we also asked if the physical localization of ASIC1a in mitochondria is necessary for this crosstalk.

We found that in cultured mouse primary cortical neurons, physiologically relevant pH decrease from 7.4 to 7.0 triggers ASIC1a dependent cytosolic Na⁺ and Ca²⁺ waves that are propagated to the mitochondria. ASIC1a inhibition by ASIC1a specific inhibitor - Psalmotoxin 1 (PcTX1) or ASIC1a gene knockout blocked these mitochondrial Na⁺ and Ca²⁺ signals. Importantly, physiological activation of ASIC1a by shifting pH from 7.4 to 7.0 enhances basal, maximal and ATP-coupled respiration. Finally, analysis of digitonin-permeabilized neurons show that PcTX1 partially reduces the pH 7.0 - evoked mitochondrial Na⁺ signaling, indicating that both plasma membrane and mitochondrion-localized ASIC1a may be involved in transmitting the signals. Altogether our results indicate that ASIC1a is critical in linking physiological mild changes of extracellular pH to mitochondrial ion signaling and metabolic activity and is therefore an important metabolic sensor.

Materials and methods

Primary neuronal culture

C57BL6 wild-type (WT) (Envigo) 7-20 weeks old pregnant female mice were obtained from Harlan Laboratories and they were maintained as previously described (Gitler, Takagishi et al. 2004). ASIC1a KO mice were kind gifts of Prof. Michael J. Welsh (Howard Hughes Medical Institute, University of Iowa, Iowa City, IA, USA) and they were generated and maintained as previously described (Wemmie, Chen et al. 2002). Animals were treated with the approvals and in accordance with the guidelines of the Ben-Gurion University Institutional Committee for Ethical Care and Use of Animals (Reference Number: IL 07-02-2019C) and in Research and the Animal Ethics Committee of Shanghai Jiao Tong University School of Medicine (Reference number: DLAS-MP-ANIM.01-05).

Briefly, mice were housed in specific pathogen free facilities. Rodent care practices were under sterile conditions, with sterile supplies. Rodents housing conditions are: 12:12 light:dark cycles at 20–24°C and 30–70% relative humidity. Animals are free fed autoclaved rodent chow and have free access to reverse osmosis filtered water. Rodents are housed in individually ventilated GM500 (Tecniplast, Italy) cages in groups of maximum 5 mice per one cage.

Primary culture of cortical neurons was done for each independent experiment from mice that were euthanized in accordance with the guidelines of the Ben-Gurion University Institutional Committee for Ethical Care and Use of Animals and Research and the Animal Ethics Committee of Shanghai Jiao Tong University School of Medicine, to minimize pain and suffering as described before (Roustan, Perrin et al. 2012). Glass coverslips (13mm, Thermo Scientific, cat # BNCB00130RA1N) placed individually into wells of a 24 well plate or glass bottom dishes (Glass Bottom Dish/29mm Dish with 14mm Bottom Well #0 Glass, Vendor: Cellvivo Cat #D29-14-0-N) were coated with poly-D-lysine (Thermo Fisher Scientific, Cat #A3890401) overnight. Planting glass surfaces were washed with sterile double distilled water and stored protected from light for less than 24 hours prior to cell seeding. Pregnant females were sacrificed on the day of culture preparation. Each pregnant female was euthanized in the sealed plastic chamber by 5% isoflurane (USP Terrel Piramal, Cat #NDC 66794-017-10), prior to the dissection of the uterus and separation of embryos (E15-16) as previously described (Roustan, Perrin et al. 2012). Isoflurane was chosen as an

inhalational anesthetic agent because of its properties to decrease pain and distress in mice. One to three embryos from one pregnant mouse were used for single culture preparation. The entire study used a total of 134 pregnant females.

The cortex was carefully dissected and separated from the rest of the brain. The dissected tissues were treated with digestion solution {4 ml HBSS (Biological Industry, Cat # 02-015-1B), 20 mM HEPES (BioLab, Cat # 000804239100) pH 7.4, 75 μ l 100 mM CaCl₂ (Sigma-Aldrich, Cat #C4901), 50 μ l 50 mM EDTA (Sigma-Aldrich, Cat #E5134 pH 7.4), cysteine crystals (Sigma Aldrich Cat #C7352) and 100 units papain (Worthington, Lakewood, Cat #LS003126)} at room temperature for 20 minutes and serially triturated. The dissociated neurons were plated onto the coated glass coverslips at the amount of 50,000-70,000 neurons per well. Neurons were plated in plating medium consisting of Neurobasal-A medium (Thermo Fisher Scientific, Cat #21103049) supplemented with 5% defined fetal bovine serum (FBS, Hyclone Life Science, Cat #SH30070.03), 2% B27 (Thermo Fisher Scientific, Cat #17504044), 2 mM Glutamax I (Life Technologies, Cat #35050038), and 1 μ g/ml gentamicin (Thermo Fisher Scientific, Cat #15750060). After 24 hours, the plating medium was replaced by a serum-free culture medium consisting of Neurobasal-A, 2% B27 and 2 mM Glutamax I. Cultures were typically maintained at 37°C in a 5% CO₂ humidified incubator for 10-15 days before experimentation using intact or permeabilized (see permeabilization protocol) neurons. Neurons were easily distinguishable from glia: they appeared phase bright, had smooth rounded somata and distinct processes, and laid just above the focal plane of the glial layer.

Cell line cultures

HEK293-T (human embryonic kidney) cell line was obtained from American Type Culture Collection (ATCC, Cat #CRL-3216, RRID: CVCL_0063) and used until 10-15 passages. This cell line was chosen because of its good overexpression abilities. These cells were authenticated to be HEK 293-T during the current year by the Genomics Center of Biomedical Core Facility of the Technion in Haifa, Israel using Promega GenePrint 24 system. Cells were cultured in DMEM (Biological Industries, Cat #01-055-1A) supplemented with 10% FBS (Biological Industries, Cat #04-007-1A), 1% penicillin/streptomycin (Biological Industries, Cat #03-031-1B) and 2 mM L-glutamine (Biological Industries, Cat #03-020-1B), as previously described (Palty, Ohana et al. 2004).

Transfection

Transfection of HEK293-T cells was performed 48 hours prior to the experiment using the calcium phosphate precipitation protocol, as previously described (Palty, Ohana et al. 2004). Complementary DNA (cDNA) of mouse ASIC1a (GenBank accession: NM_009597.1) in pEGFP-C3 vector (Clontech, Cat #632482) as previously reported (Yu, Chen et al. 2010) was used for transfection. Control vector was pcDNA3 (Palty, Ohana et al. 2004). All custom made materials will be shared upon reasonable request.

Cell permeabilization

Primary cortical neurons and HEK293-T cells were permeabilized as described before (Roy, Dey et al. 2017). Briefly, cells were kept in a 0.007% digitonin (Sigma Aldrich, Cat #D141)

buffer containing 113 mM K-D-gluconate (Sigma Aldrich, Cat # G4500), 15 mM N-methyl-D-glucamine (NMDG⁺, Sigma-Aldrich, Cat #M2004), 6 mM MgCl₂ (Sigma-Aldrich, Cat #M9272), 20 mM HEPES, 10 mM EGTA (Gerbu, Cat #1310), with the pH adjusted to 7.4 by KOH (Sigma-Aldrich, Cat #P5958), following the addition of 15 mM Na⁺ (NaCl, Bio-Lab, Cat #001903059100) containing Ringer's solution. Ionic signals in the intact mitochondria were monitored by fluorescent imaging using mitochondrial targeting specific Na⁺ fluorescence dye, CoroNa Red (Molecular probes, Cat #C24430).

Fluorescence Imaging

Experiments done on HEK293-T cells and WT and/or PcTX1 (Alomone labs, #STP200) or Nifedipine (Sigma Aldrich, Cat #N7634) treated WT neurons were performed using the imaging system consisted of an Axiovert 100 inverted microscope (Zeiss), Polychrome V monochromator (TILL Photonics, Planegg, Germany) and a SensiCam cooled charge-coupled device (PCO, Kelheim, Germany). Cells seeded on the glass coverslips as described previously, were positioned to a special holder designed to enable constant flow of solutions without changing the definite amount of perfusion solution and thus the imaging focus. Fluorescent images were acquired with Imaging WorkBench 4.0 (Axon Instruments, Foster City, CA) using magnification of 10x for cytosolic and 20x for mitochondrial measurements. Acquisition speed was 1 frame every 3 seconds for the experiments measuring mitochondrial Ca²⁺, cytosolic and mitochondrial Na⁺, mitochondrial membrane potential, and 1 frame every 1.5 seconds for cytosolic Ca²⁺ measurements. No significant dye leak or change in viability for monitoring were recorded during our brief imaging sessions.

ASIC1a KO related experiments were done using neurons cultured on glass bottom dishes as described previously. The dish was mounted on the stage of an inverted fluorescence microscope (Nikon Eclipse TI, Japan) and neurons were observed with a 20x objective lens. The fluorescence images were acquired while neurons were continuously perfused. Puff perfusion changes were achieved with the use of the ALA-VM8 8 valve manifold for perfusion system whose tip is placed approximately 500 μm from neurons and the velocity of flow is ~350 μl/min.

In all fluorescent experiments, cells were pre-loaded with the indicated ion specific fluorescent dye at the indicated concentrations for 30 min at room temperature using Ringer's solution containing (in mM): 126 NaCl, 5.4 KCl (Sigma-Aldrich, Cat #P9333), 0.8 MgCl₂, 20 HEPES, 1.8 CaCl₂, 15 glucose (Gerbu, Cat #2028), with pH adjusted to 7.4 with NaOH (Sigma-Aldrich, Cat #221465) and supplemented with 0.1% bovine serum albumin (BSA, VWR, Cat #0332). The Na⁺ free Ringer's solution had the same composition except Na⁺ was replaced by equimolar NMDG⁺. After loading, cells were washed quickly 3 times and then incubated for 30 minutes in the dye-free Ringer's solution.

At the beginning of each experiment, cells were perfused with Ca²⁺-containing Ringer's solution supplemented with 0.1% BSA. To trigger ionic responses, cells were perfused with the Ringer's solution of the same composition but with pH adjusted to 7.0 by 32% HCl (Frutarom, Cat #55200).

Fluorescent imaging of Na⁺ in cytosol and mitochondria was performed using cells loaded with Asante NaTRIUM Green-2 AM (TefLabs, Cat #3512) (1 μM) and CoroNa Red, respectively. Cytosolic Na⁺ response was acquired in cells loaded with Asante NaTRIUM Green-2 at excitation of 488 nm and emission of 510 nm with a long pass filter. Mitochondrial Na⁺ signals were monitored in cells loaded with CoroNa Red at excitation of 568 nm and emission of 590 nm, as previously described (Nita, Hershinkel et al. 2012).

Cytosolic Ca²⁺ was monitored in cells loaded with Ca²⁺ specific ratiometric dye Fura-2-AM (Sigma Aldrich, Cat #F0888) (1 μM), which were illuminated alternately with 340 nm and 380 nm excitations and imaged with a 510 nm long pass filter. Mitochondrial Ca²⁺ was measured in cells loaded with Ca²⁺ specific dye Rhod-2 AM (Biotium, Cat #50024) (1 μM) that preferentially localizes in mitochondria. Rhod-2 was excited at 552 nm wavelength light and imaged with a 570 nm-long pass filter as previously described (Kostic, Ludtmann et al. 2015).

Mitochondrial membrane potential (Ψ_m) changes ($\Delta\Psi_m$) were monitored by detecting microfluorimetric changes in fluorescence of the membrane potential-sensitive probe Rhodamine 123 (Biotium, Cat #70010) (1.26 μM). Rhodamine 123 was excited at 490 nm and imaged with a 535 nm emission filter as previously described (Beckervordersandforth, Ebert et al. 2017). Note that mitochondrial depolarization is showed as a rise in fluorescence when Rhodamine 123 is used. FCCP (Sigma Aldrich, Cat #C2920) was added in the end of each experiment to induce complete depolarization ($F_{\max} = F_{\text{FCCP}} - F_0$). Fluorescence traces were normalized to F_{\max} .

PcTX1 treatment was performed prior to each fluorescent imaging experiment for 120 s in a concentration of 20 nM, known to block ASIC1a (Wang, Wang et al. 2015)

Oxygen Consumption measurements

Primary cultured cortical neurons were seeded onto poly-D-lysine-coated 24-well seahorse plates (Agilent, Cat #100777-004) immediately after isolation. Neurons were plated in planting medium for the first 24 hours when the medium was partly replaced with serum-free culture medium. Cultures were typically maintained at 37°C in a 5% CO₂ humidified incubator for 10-15 days before experimentation. At 24 hours before the experiment, cartridge was immersed in XF calibrant solution (Agilent, Cat #100840-000) and placed in a CO₂ free incubator until used. Seahorse working protocol was carried out as described before (Cerqueira, Chausse et al. 2016). Briefly, on the day of the experiment, two hours before oxygen consumption measurements, medium was replaced by low glucose assay medium (2.4 mM glucose, 0.8 mM MgCl₂, 1.8 mM CaCl₂, 143 mM NaCl, 5.4 mM KCl, 0.91 mM NaH₂PO₄ (Sigma-Aldrich, Cat #S97663) and 15 mg/ml phenol red (Sigma, Cat #P0290) and neurons were kept at 37°C without CO₂, to evoke glycolysis. During these two hours, ports of cartridge containing the oxygen probes were loaded with the compounds to be injected during the assay (50 μl per port) and the cartridge was calibrated. Neurons treated with PcTX1 were kept in toxin containing media for 120 sec with a final concentration of 20 nM PcTX1 and then washed with the toxin-free assay media. Basal respiration was recorded for 20 min, at 5 min intervals, until system stabilization. FCCP was used at a final concentration of 1 μM and injected with sodium pyruvate (Sigma-Aldrich, Cat

#P2256) at a final concentration of 5 mM. Oligomycin (Sigma-Aldrich, Cat #75351) and antimycin (Sigma Aldrich, Cat #A8674) were used at final concentrations of 1 μ M and 4 μ M, respectively. All respiratory modulators were used at optimal concentrations titrated during preliminary optimization experiments (data not shown). The assay was performed using Seahorse Bioscience XF96 extracellular flux analyzer and the statistics were exported from the Wave (Seahorse official) software.

Immunoblot analysis

Immunoblot analysis were performed using anti-ASIC1a primary antibodies, as described previously (Wang, Zeng et al. 2013). Briefly, mouse cortexes or cell pellets were collected and re-suspended in a lysis buffer containing 20 mM Tris-Cl (pH 7.4, Bio-Lab, Cat #002009239100), 150 mM NaCl, 1% Triton X-100 (Bio-Lab, Cat #20180501), 1 mM EDTA, 3 mM NaF (Sigma-Aldrich, Cat #S7920), 1 mM β -glycerophosphate (Sigma Aldrich, Cat #G9422), 1 mM sodium orthovanadate (Sigma-Aldrich, Cat #S6508), 10% glycerol (Sigma-Aldrich, Cat #G7757) and complete protease inhibitor set (Sigma-Aldrich, Cat #P2714). The re-suspended lysates were vortexed for 20 sec, incubated on ice for 30 min and centrifuged at 13000 r.p.m. for 15 min. The supernatants were collected for Western blot analysis. Protein concentration was determined by Bradford procedure, according to the manufacturer's protocol (Bio-Rad, Cat #500-0006). Equal amounts of proteins (10 μ g) were run on 10% SDS-PAGE and transferred to a PVDF membrane (ISEQ00010, Immobilon-PSQ Membrane). The membranes were blocked by 5% skimmed milk powder (PLYGEN, Cat #P1622) dissolved in TBST washing buffer (Sangon Biotech, Cat #C520009-0500) and then incubated with anti ASIC1a antibody (1:500, Santa Cruz Biotechnology, Cat #sc-13905) overnight at 4 °C. Immunoblots were processed with corresponding secondary antibodies Rb x Gt IgG HRP (1:2000) (EMD Millipore Corp, Cat #AP106P) for 2 h at room temperature. Immunoblots were probed and the bands were visualized with enhanced chemiluminescence on ImageQuant LAS 4000 mini (GE Healthcare Life Sciences).

PCR analysis

PCR analysis were provided as described before (Wemmie, Chen et al. 2002) using the official genotyping protocol provided by Jackson Laboratories. Primers used were: ASIC1a_1: 5'-CCG CCT TGA GCG GCA GGT TTA AAG G-3'; ASIC1a_2: 5'-CAT GTC ACC AAG CTC GAC GAG GTG-3'; ASIC1a_3: 5'-TGG ATG TGG AAT GTG TGC GA-3' and PCR procedure was: Step1: Pre-denaturation 94°C 2 min, Step2: Denaturation 94°C 20 s, Step3: Annealing 59°C 20 s, Step4: Extension 68°C 40 s, Step5: Repeat step 2-4, 34 times, Step6: 72°C 5 min, Step7: 10°C ∞ .

Statistical analysis

For all single-cell imaging experiments, traces of average responses, recorded from 5 to 20 cells in each independent cell culture preparation (n), in a non-blind manner were analyzed and plotted using KaleidaGraph. No randomization or sample size calculation was performed and the study was not preregistered. The study was exploratory and no exclusion of data was predetermined or performed. The rate of Na⁺ and Ca²⁺ transport was derived by a linear fit of the change in the fluorescence (ΔF) over a period of 10-20 s following initiation of apparent efflux/influx ($\Delta F/\Delta t$) from each graph. Rates from n experiments (as

described in legends to the figures) were averaged and displayed in bar graph format (mean \pm SEM). GraphPad Prism 6 software was used for statistical analysis and Adobe Illustrator for the graphic design of the figures. All bar graphs were presented as averaged values from independent measurements \pm SEM and data were compared using Student's t test. A level of $p < 0.05$ was accepted as statistically significant. Symbols of significance used: ns $p > 0.05$, * $p < 0.05$, ** $p < 0.01$, *** $p < 0.001$, **** $p < 0.0001$.

Results

ASIC1a has been well-known to play a major pathological role under conditions of brain injury such as ischemic stroke when extra-neuronal pH drops drastically to around pH 6.0. However, in which way ASIC1a contributes to metabolic processes during normal physiological brain activity, which can also produce small extracellular pH (pH_e) decreases to around pH 7.0, remains unclear. Here, we focused on the effects of this mild pH drop on the crosstalk of ASIC1a with the mitochondrial Na^+ and Ca^{2+} signaling as well as the mitochondrial metabolic rate.

We first asked if a change of pH_e from 7.4 to 7.0 could trigger an ASIC1a-dependent cytosolic Na^+ signal in neurons. We applied the pH 7.0 solution either through superfusion or direct pressure ejection (puffing). In the former case, primary cultured mouse cortical neurons loaded with the cytosolic fluorescent Na^+ reporter, Asante NaTRIUM Green-2, were superfused with Ringer's solution of pH 7.4 and then the perfusate was switched to the same Ringer's solution of pH 7.0 to activate ASIC1a. The shift from pH 7.4 to 7.0 evoked a massive influx of Na^+ , which was largely suppressed by the inclusion of the ASIC1a antagonist, PcTX1 (Figure 1 A-B), indicating that activation of ASIC1a by this 0.4 pH unit drop was sufficient to evoke Na^+ influx. Then, we monitored changes in cytosolic Na^+ levels in neurons that received direct puffing of the pH 7.0 solution (Figure 1 C-D). In wild type (WT) mouse cortical neurons, puffing the pH 7.0 solution elicited an even faster cytosolic Na^+ rise than superfusion (compared to Figure 1 A-B); however, this increase in cytosolic Na^+ was absent in neurons prepared from ASIC1a KO (Figure 1E) mice (Figure 1 C-D). These results indicate that the small 0.4 pH unit decrease is sufficient to trigger ASIC1a activation, causing a massive Na^+ influx into the cytosol. To further interrogate the role of ASIC1a in generating the Na^+ signals, we subjected HEK293-T cells that overexpressed ASIC1a (Figure 1F) to the same experimental paradigm described in figure 1A. Consistent with the results presented in figures 1 A-D, ASIC1a dependent cytosolic Na^+ rise occurred immediately following the switch of perfusate pH from 7.4 to 7.0 in HEK293-T cells overexpressing ASIC1a, which was again largely attenuated by PcTX1 (Figure 1 G-H). Note that we observed an increase of cytosolic Na^+ signal in control consistent with the endogenous expression of ASIC1a in HEK293-T cells (Gunthorpe, Smith et al. 2001)

Next, to examine if the cytosolic Na^+ rise mediated by ASIC1a is followed by mitochondrial Na^+ signals, we monitored mitochondrial Na^+ concentration changes in neurons loaded with the mitochondrial Na^+ dye Corona Red (Figure 1 J-K). With the pH_e shifted from 7.4 to 7.0, a rise in mitochondrial Na^+ concentration was observed, which was partially blocked by PcTX1, indicating that the cytosolic Na^+ rise mediated by ASIC1a is propagated into the mitochondria.

We then sought to determine if the activation of ASIC1a at a physiological pH change could affect the mitochondrial metabolic activity. To do this, we monitored mitochondrial membrane potential changes in neurons loaded with the mitochondrial membrane potential dye Rhodamine 123. Indeed, the shift of pH_e from 7.4 to 7.0 either through superfusion or puffing was followed by a partial mitochondrial depolarization, which was largely suppressed by PcTX1 (Figure 2 A-B) and completely abolished by the knockout of *Asic1a* gene (Figure 2 C-F). These results show that there is a crosstalk between ASIC1a and mitochondria that regulates the mitochondrial membrane potential under physiological pH changes. As in the previous experimental set up, we also checked how ASIC1a overexpression affects mitochondrial membrane potential in HEK293-T cells. As expected, overexpressed ASIC1a increased the depolarization response of mitochondrial membranes to the mild extracellular acidification (Figure 2 D-E).

Calcium is an important regulator of mitochondrial metabolic activity and its mitochondrial transients thus determines the temporal control of mitochondrial signaling. We therefore aimed to determine if the crosstalk of ASIC1a with mitochondria involves mitochondrial Ca^{2+} transients. To this end, we first monitored cytosolic Ca^{2+} changes in neurons loaded with Fura-2-AM (Figure 3). With the pH_e lowered from 7.4 to 7.0 by either superfusion (Figure 3A-C) or puffing (Figure 3B-D), we observed robust increases in cytosolic Ca^{2+} signals in WT neurons. The increase was markedly inhibited by PcTX1 (Figure 3 A-E) and completely missing in ASIC1a KO neurons (Figure 3 B-F). We next monitored changes of mitochondrial Ca^{2+} signals in response to the pH_e shift from 7.4 to 7.0 in neurons that were loaded with the mitochondrial Ca^{2+} indicator Rhod-2 (Figure 3 C-D). Again, the mild pH_e decrease was followed by a robust mitochondrial Ca^{2+} transient, which was largely blocked by the ASIC1a inhibitor PcTX1 and completely lacking in ASIC1a KO neurons (Figure 3 H-I). With the pH_e switch made through puffing, the mitochondrial Ca^{2+} rise acquired higher levels than that made via superfusion (compare Figure 3 C-H to 3 D-I), reminiscent of the faster cytosolic Na^+ concentration rise induced by puffing than superfusion (see Figure 1 A-C). To ascertain that the mild pH_e drop-induced mitochondrial Ca^{2+} transient is indeed augmented by ASIC1a, we compared the magnitudes of mitochondrial Ca^{2+} transients in HEK293-T cells that overexpressed ASIC1a with that transfected by the empty vector (pcDNA3). Consistent with the results presented in Figure 1 J-K, increasing ASIC1a expression resulted in higher pH 7.0-evoked mitochondrial Ca^{2+} transients (Figure 3 K-L).

Although the level of ASIC1a in HEK293-T cells due to ectopic expression should be higher than that in native neurons, the ASIC1a dependent Ca^{2+} concentration rise in mitochondria was greater in neurons than in transfected HEK293-T cells (Figure 3 K-L). We reasoned that in neurons the ASIC1a-triggered Ca^{2+} response might include a contribution of voltage-gated Ca^{2+} channel. Therefore, we examined the mitochondrial Ca^{2+} response in the presence of a L-type Ca^{2+} channel blocker, nifedipine, and found that nifedipine indeed suppressed about half of the pH 7.0-evoked mitochondrial Ca^{2+} response, contrasted with the nearly complete inhibition by PcTX1 (Figure 3M-N). Consistent with previous studies that L-type Ca^{2+} channels have a significant effect in amplifying the ASIC1a dependent Ca^{2+} response (Cheng, Chen et al. 2015), our results indicate that in neurons Ca^{2+} signal was further enhanced by activation of the voltage-gated Ca^{2+} channels (see discussion). Altogether our findings show that the mild extracellular pH decrease evokes cytosolic Na^+

and Ca^{2+} responses, initiated by ASIC1a and presumably amplified by the voltage-gated Ca^{2+} channels, which are then subsequently communicated to the mitochondria.

Furthermore, to determine if the crosstalk between ASIC1a and mitochondria changes mitochondrial metabolic activity, we performed Seahorse metabolic analysis (Figure 4). We found that the evoked glycolysis triggered a drop of pH_e from 7.4 to ~6.5 (Figure 4A) and hence enhanced basal and maximal respiration as well as ATP production (Figure 4 B-E). The enhanced respiration was blocked by PcTX1 (Figure 4 B-C) and was lower in ASIC1a KO compared to WT neurons (Figure 4 D-E).

Finally, our group recently found that ASIC1a is not only expressed on the plasma membrane but also an integral part of mitochondrial membrane (Wang, Zeng et al. 2013). To determine if the mitochondrial resident ASIC1a is involved in mediating mitochondrial Na^+ uptake in response to the low pH_e change, we monitored mitochondrial Na^+ signals in Corona red - preloaded cells that were permeabilized with digitonin (See Materials and methods). We found that mitochondrial Na^+ signal was evoked by the pH_e shift from 7.4 to 7.0 in HEK293-T cells that overexpressed ASIC1a and the response was decreased by pre-treatment of cells with PcTX1 (Figure 5 A-B). Likewise, a similar pH_e decrease also evoked mitochondrial Na^+ signals in digitonin-permeabilized neurons, which was partially sensitive to the block by PcTX1 (Figure 5 C-D). Note the decrease in the rate of mitochondrial Na^+ influx in PcTX1 pre-treated compared to untreated neurons (Figure 5 C-D)

Altogether, our results indicate that a crosstalk between ASIC1a and mitochondria induced by mild extracellular pH drop plays a key role in controlling metabolic activity of neurons, and both the plasma membrane and mitochondrial membrane localized ASIC1a participate in this crosstalk .

Discussion

ASIC1a has been studied in the context of large extracellular pH changes such as during synaptic transmission when protons are co-released from the presynaptic site with the neurotransmitters or in pathophysiological acidosis occurring during ischemia and many forms of neurodegeneration (Wemmie, Chen et al. 2002, Tian, Wang et al. 2016). However, little is known about the role of ASIC1a during mild pH fluctuations associated with normal physiological metabolism. This study shows that ASIC1a-dependent cytosolic and mitochondrial Na^+ and Ca^{2+} fluxes are evoked by physiological pH changes. Inhibition by PcTX1 and knocking out of *Asic1a* gene significantly attenuated pH 7.0 evoked - Na^+ signals in neurons, both in the cytosol and mitochondria. Additionally, Ca^{2+} transients were strongly reduced in both compartments upon blocking ASIC1a by the toxin or in ASIC1a KO neurons. Our data further demonstrate that ASIC1a plays a role in controlling mitochondrial membrane potential, suggesting that it has physiological implications on mitochondrial metabolic activity. The novel insight of the ASIC1a role in the physiological processes of neurons is supported by our major finding that mitochondrial respiration is decreased in ASIC1a inhibited or deficient neurons. Taken together, we suggest that ASIC1a is a physiological metabolic sensor that by communicating with mitochondria, reinforces

mitochondrial respiration and thereby upregulates mitochondrial energy metabolism in neurons (Figure 6).

Notably the Ca^{2+} permeation of ASIC1a is rather modest (Grunder and Chen 2010, Grunder and Pusch 2015, Waldmann, Champigny et al. 1997). How can this small permeation be consistent with the large Ca^{2+} influx and the mitochondrial Ca^{2+} signals that we detected in neurons? Activation of ASIC1a triggers large Na^+ influx leading to neuronal depolarization thereby further augmentation of cation permeation via voltage-gated Na^+ and/or Ca^{2+} channels (VGSC and VGCC) that are ubiquitously expressed in neurons. Such concerted process initiated by ASIC1a followed by the Ca^{2+} and Na^+ channels can lead to the large Ca^{2+} and Na^+ signals that we observed (Figure 1 and 3).

We show that neuronal ASIC1a is involved in cytosolic and mitochondrial Na^+ signaling even following a mild pH_e change. A pH_e shift from 7.4 to 7.0 was sufficient to trigger a cytosolic Na^+ rise that was propagated to mitochondria. Both cytosolic and mitochondrial Na^+ transients were blocked by PcTX1. To address the role of ASIC1a in this process more specifically, we employed ASIC1a KO mouse model. A direct puff of pH 7.0 solution onto the WT neurons triggered Na^+ and Ca^{2+} increase in cytosol, while the signal was absent in ASIC1a KO neurons (Figure 1 and 3). The major role of ASIC1a in controlling Na^+ signaling is underscored by the striking reduction in cytosolic Na^+ response in ASIC1a KO neurons when pH_e was switched from 7.4 to 7.0 (Figure 1). When overexpressed in HEK293-T cells, ASIC1a mediated pH 7.0-induced cytosolic Na^+ rise (Figure 1). Of interest was the larger cytosolic Na^+ and mitochondrial Ca^{2+} responses seen in WT neurons using the direct puff of the acidic solution than superfusion with acidic buffer. Although the reason for such differences is not entirely clear, the abrupt pH change achieved by puffing probably induced more synchronized ASIC1a activation than the slow exchange by superfusion. Since ASIC1a channel desensitizes rapidly (Kellenberger and Schild 2015), the simultaneous activation of all the ASIC1a channels in the cell is expected to cause more robust Na^+ influx than the unsynchronized activation. Consistent with this idea, we have previously shown that the perfusion rate strongly impacts the pH 6.0 solution-evoked Ca^{2+} signals via ASIC1a (Wang, Wang et al. 2015). Here, given that the mitochondrial Ca^{2+} response was enhanced by puffing the pH 7.0 solution that impacted the increase in cytosolic Na^+ , rather than Ca^{2+} , it is possible that the cytosolic Na^+ signal plays a major role in causing the mitochondrial Ca^{2+} increase under the mild pH drop. It will be of interest to determine if other isoforms of ASICs (ASIC2 or ASIC3), which are Ca^{2+} -impermeable, could produce a similar effect and at what pH_e values.

Several pathways control Na^+ permeation into mitochondria. Among them, the most notable ones are mitochondrial $\text{Na}^+/\text{Ca}^{2+}$ exchanger (NCLX) (Palty, Silverman et al. 2010) and mitochondrial Na^+/H^+ exchanger (Numata, Petrecca et al. 1998). By propagating Na^+ signal from cytosol to mitochondria we show for the first time that the ASIC1a-dependent cytosolic Na^+ signal is propagated to mitochondria in intact neurons (Figure 1). We further demonstrate that the activation of ASIC1a leads to mitochondrial depolarization thereby controlling the metabolic activity of this organelle. ASIC1a activation by mild pH drop triggers mitochondrial membrane depolarization in WT neurons and in ASIC1a overexpressed HEK293-T cells (Figure 2). No change in mitochondrial membrane potential

is detected in ASIC1a KO neurons upon application of pH 7.0 (Figure 2). Importantly, application of the mitochondrial uncoupler, FCCP, revealed that in ASIC1a KO neurons mitochondria are intact.

Mitochondrial membrane potential changes may be associated with Ca^{2+} permeation into mitochondria. Here we demonstrate that ASIC1a dependent mitochondrial depolarization is indeed accompanied by mitochondrial Ca^{2+} signal in WT neurons, which is abolished in ASIC1a inhibited/KO neurons (Figure 3). To support this hypothesis, we also show that ASIC1a overexpression and activation by pH 7.0 induce mitochondrial Ca^{2+} rise in HEK293-T cells (Figure 3).

In pathophysiological scenarios of tissue acidosis ASIC1a is known to play a critical role in brain damage and causes neurological deficits (Xiong, Zhu et al. 2004). Here we demonstrate that mild physiological pH changes also activate ASIC1a, leading to enhanced Na^+ and Ca^{2+} signaling which, if prolonged, might result in continuous mitochondrial Ca^{2+} uptake. Such scenario can on one hand enhance metabolic activity of neurons (Griffiths and Rutter 2009, Rizzuto, Bastianutto et al. 1994, Jouaville, Pinton et al. 1999), linking ASIC1a activation to accelerated mitochondrial activity. On the other hand, excessive and/ or extended ASIC1a activation might lead to activation of mitochondrial permeability transition pore (mPTP), which could culminate in neuronal death (Bernardi and Rasola 2007).

Previously, we have shown that in addition to working as a plasma membrane channel, ASIC1a is also present in the inner mitochondrial membrane and physically associated with mPTP, where it plays a critical role in oxidation-induced cell death (Wang, Zeng et al. 2013). However, whether or not the mitochondrial ASIC1a (mtASIC1a) functions as an ion channel remained elusive. Here we show that most likely mtASIC1a acts as a channel that mediates mitochondrial Na^+ influx. In both permeabilized HEK293-T cells that overexpress ASIC1a and primary cortical neurons, mitochondrial Na^+ signal triggered by pH 7.0 is mediated by channels sensitive to PcTX1, suggesting that these Na^+ signals are at least in part, mediated by mtASIC1a (Figure 5). Therefore, mtASIC1a might be directly involved in control of mitochondrial membrane potential and mitochondrial metabolic activity in addition to its role in regulating mPTP and cell demise. Although it is not entirely clear how cell membrane ASIC1a communicate with mitochondrial ASIC1a, we propose that the Na^+ and Ca^{2+} fluxes triggered by the former are propagated to the latter on the mitochondria and are facilitated by the lower pH of the cytoplasm.

Our findings suggest that ASIC1a is activated by a mild and physiologically relevant extracellular pH drop, which is followed by direct ASIC1a-mediated Na^+ and Ca^{2+} concentration increases both in cytosol and mitochondria. The ASIC1a-dependent Ca^{2+} response is further supported by our finding that it triggered Ca^{2+} signals in ASIC1a-overexpressing HEK293-T cells, which do not express VGCC (Berjukow, Doring et al. 1996). Next, by the Na^+ and/or Ca^{2+} -evoked mitochondrial membrane depolarization and mitochondrial Na^+ and Ca^{2+} transient propagated from the cytosol, the activation of ASIC1a increases the mitochondrial respiration and mitochondrial metabolic activity. Our results therefore suggest a new communication pathway between plasmalemmal ASIC1a and

mitochondria. Finally, we demonstrate the role of mtASIC1a as a Na⁺ channel, which can additionally affect mitochondrial signaling and metabolic properties.

Acknowledgments

This study was supported by grants from the National Natural Science Foundation of China (81730095 and 31461143004) to T.L.X., the Science and Technology Commission of Shanghai Municipality (18JC1420302) to T.L.X., the Shanghai Municipal Science and Technology Major Project (2018SHZDZX05) to T.L.X., NIH (NS102452) to M.X.Z. and ISF China (1210/14) to T.L.X. and I.S. We would like to thank Dr. Marko Kostic for scientific discussions and Maya Rozenfeld for neuronal culture preparation.

List of abbreviations

ASIC	acid sensing ion channel
NCLX	Na ⁺ /Ca ²⁺ exchanger
PcTX1	psalmotoxin 1
RRID	Research Resource Identifier

References

- Askwith CC, Wemmie JA, Price MP, Rokhlina T and Welsh MJ (2004). "Acid-sensing ion channel 2 (ASIC2) modulates ASIC1 H⁺-activated currents in hippocampal neurons." *J Biol Chem* 279(18): 18296–18305. [PubMed: 14960591]
- Berjukow S, Doring F, Froschmayr M, Grabner M, Glossmann H and Hering S (1996). "Endogenous calcium channels in human embryonic kidney (HEK293) cells." *Br J Pharmacol* 118(3): 748–754. [PubMed: 8762103]
- Bernardi P and Rasola A (2007). "Calcium and cell death: the mitochondrial connection." *Subcell Biochem* 45: 481–506. [PubMed: 18193649]
- Cheng J, Chen Y, Xing H, Jiang H and Ye X (2015). "Down-regulation of ASICs current and the calcium transients by disrupting PICK1 protects primary cultured mouse cortical neurons from OGD-Rep insults." *Int J Clin Exp Pathol* 8(9): 10272–10282. [PubMed: 26617735]
- Chiang PH, Chien TC, Chen CC, Yanagawa Y and Lien CC (2015). "ASIC-dependent LTP at multiple glutamatergic synapses in amygdala network is required for fear memory." *Sci Rep* 5: 10143. [PubMed: 25988357]
- Coryell MW, Wunsch AM, Haeflner JM, Allen JE, McBride JL, Davidson BL and Wemmie JA (2008). "Restoring Acid-sensing ion channel-1a in the amygdala of knock-out mice rescues fear memory but not unconditioned fear responses." *J Neurosci* 28(51): 13738–13741. [PubMed: 19091964]
- Gitler D, Takagishi Y, Feng J, Ren Y, Rodriguiz RM, Wetsel WC, Greengard P and Augustine GJ (2004). "Different presynaptic roles of synapsins at excitatory and inhibitory synapses." *J Neurosci* 24(50): 11368–11380. [PubMed: 15601943]
- Griffiths EJ and Rutter GA (2009). "Mitochondrial calcium as a key regulator of mitochondrial ATP production in mammalian cells." *Biochim Biophys Acta* 1787(11): 1324–1333. [PubMed: 19366607]
- Grifoni SC, Jernigan NL, Hamilton G and Drummond HA (2008). "ASIC proteins regulate smooth muscle cell migration." *Microvasc Res* 75(2): 202–210. [PubMed: 17936312]
- Grunder S and Chen X (2010). "Structure, function, and pharmacology of acid-sensing ion channels (ASICs): focus on ASIC1a." *Int J Physiol Pathophysiol Pharmacol* 2(2): 73–94. [PubMed: 21383888]
- Grunder S and Pusch M (2015). "Biophysical properties of acid-sensing ion channels (ASICs)." *Neuropharmacology* 94: 9–18. [PubMed: 25585135]

- Gunthorpe MJ, Smith GD, Davis JB and Randall AD (2001). "Characterisation of a human acid-sensing ion channel (hASIC1a) endogenously expressed in HEK293 cells." *Pflugers Arch* 442(5): 668–674. [PubMed: 11512022]
- Jahr H, van Driel M, van Osch GJ, Weinans H and van Leeuwen JP (2005). "Identification of acid-sensing ion channels in bone." *Biochem Biophys Res Commun* 337(1): 349–354. [PubMed: 16185661]
- Jouaville LS, Pinton P, Bastianutto C, Rutter GA and Rizzuto R (1999). "Regulation of mitochondrial ATP synthesis by calcium: evidence for a long-term metabolic priming." *Proc Natl Acad Sci U S A* 96(24): 13807–13812. [PubMed: 10570154]
- Kellenberger S and Schild L (2015). "International Union of Basic and Clinical Pharmacology. XCI. structure, function, and pharmacology of acid-sensing ion channels and the epithelial Na⁺ channel." *Pharmacol Rev* 67(1): 1–35. [PubMed: 25287517]
- Liu G, Yan G, Zhu B and Lu L (2016). "Design of a video capsule endoscopy system with low-power ASIC for monitoring gastrointestinal tract." *Med Biol Eng Comput* 54(11): 1779–1791. [PubMed: 27016367]
- McCormack JG and Denton RM (1990). "The role of mitochondrial Ca²⁺ transport and matrix Ca²⁺ in signal transduction in mammalian tissues." *Biochim Biophys Acta* 1018(2-3): 287–291. [PubMed: 2203475]
- Numata M, Petrecca K, Lake N and Orłowski J (1998). "Identification of a mitochondrial Na⁺/H⁺ exchanger." *J Biol Chem* 273(12): 6951–6959. [PubMed: 9507001]
- Palty R, Silverman WF, Hershinkel M, Caporale T, Sensi SL, Parnis J, Nolte C, Fishman D, Shoshan-Barmatz V, Herrmann S, Khananshvili D and Sekler I (2010). "NCLX is an essential component of mitochondrial Na⁺/Ca²⁺ exchange." *Proc Natl Acad Sci U S A* 107(1): 436–441. [PubMed: 20018762]
- Pellerin L, Pellegrini G, Bittar PG, Charnay Y, Bouras C, Martin JL, Stella N and Magistretti PJ (1998). "Evidence supporting the existence of an activity-dependent astrocyte-neuron lactate shuttle." *Dev Neurosci* 20(4-5): 291–299. [PubMed: 9778565]
- Rizzuto R, Bastianutto C, Brini M, Murgia M and Pozzan T (1994). "Mitochondrial Ca²⁺ homeostasis in intact cells." *J Cell Biol* 126(5): 1183–1194. [PubMed: 8063855]
- Roustan A, Perrin J, Berthelot-Ricou A, Lopez E, Botta A and Courbiere B (2012). "Evaluating methods of mouse euthanasia on the oocyte quality: cervical dislocation versus isoflurane inhalation." *Lab Anim* 46(2): 167–169. [PubMed: 22511734]
- Tian L, Wang JH, Zhao M, Bao YC, Shang JF, Yan Q, Zhang ZC, Du XZ, Jiang H, Sun RJ, Yuan B, Zhang XH, Zhang TZ and Li XL (2016). "[Effect of Scalp-acupuncture Stimulation on Neurological Function and Expression of ASIC 1 a and ASIC 2 b of Hippocampal CA 1 Region in Cerebral Ischemia Rats]." *Zhen Ci Yan Jiu* 41(5): 417–422. [PubMed: 29071942]
- Waldmann R, Champigny G, Bassilana F, Heurteaux C and Lazdunski M (1997). "A proton-gated cation channel involved in acid-sensing." *Nature* 386(6621): 173–177. [PubMed: 9062189]
- Wang YZ, Zeng WZ, Xiao X, Huang Y, Song XL, Yu Z, Tang D, Dong XP, Zhu MX and Xu TL (2013). "Intracellular ASIC1a regulates mitochondrial permeability transition-dependent neuronal death." *Cell Death Differ* 20(10): 1359–1369. [PubMed: 23852371]
- Wemmie JA, Chen J, Askwith CC, Hruska-Hageman AM, Price MP, Nolan BC, Yoder PG, Lamani E, Hoshi T, Freeman JH Jr. and Welsh MJ (2002). "The acid-activated ion channel ASIC contributes to synaptic plasticity, learning, and memory." *Neuron* 34(3): 463–477. [PubMed: 11988176]
- Wu LJ, Duan B, Mei YD, Gao J, Chen JG, Zhuo M, Xu L, Wu M and Xu TL (2004). "Characterization of acid-sensing ion channels in dorsal horn neurons of rat spinal cord." *J Biol Chem* 279(42): 43716–43724. [PubMed: 15302881]
- Xiong ZG, Zhu XM, Chu XP, Minami M, Hey J, Wei WL, MacDonald JF, Wemmie JA, Price MP, Welsh MJ and Simon RP (2004). "Neuroprotection in ischemia: blocking calcium-permeable acid-sensing ion channels." *Cell* 118(6): 687–698. [PubMed: 15369669]
- Zima AV, Pabbidi MR, Lipsius SL and Blatter LA (2013). "Effects of mitochondrial uncoupling on Ca(2+) signaling during excitation-contraction coupling in atrial myocytes." *Am J Physiol Heart Circ Physiol* 304(7): H983–993. [PubMed: 23376829]

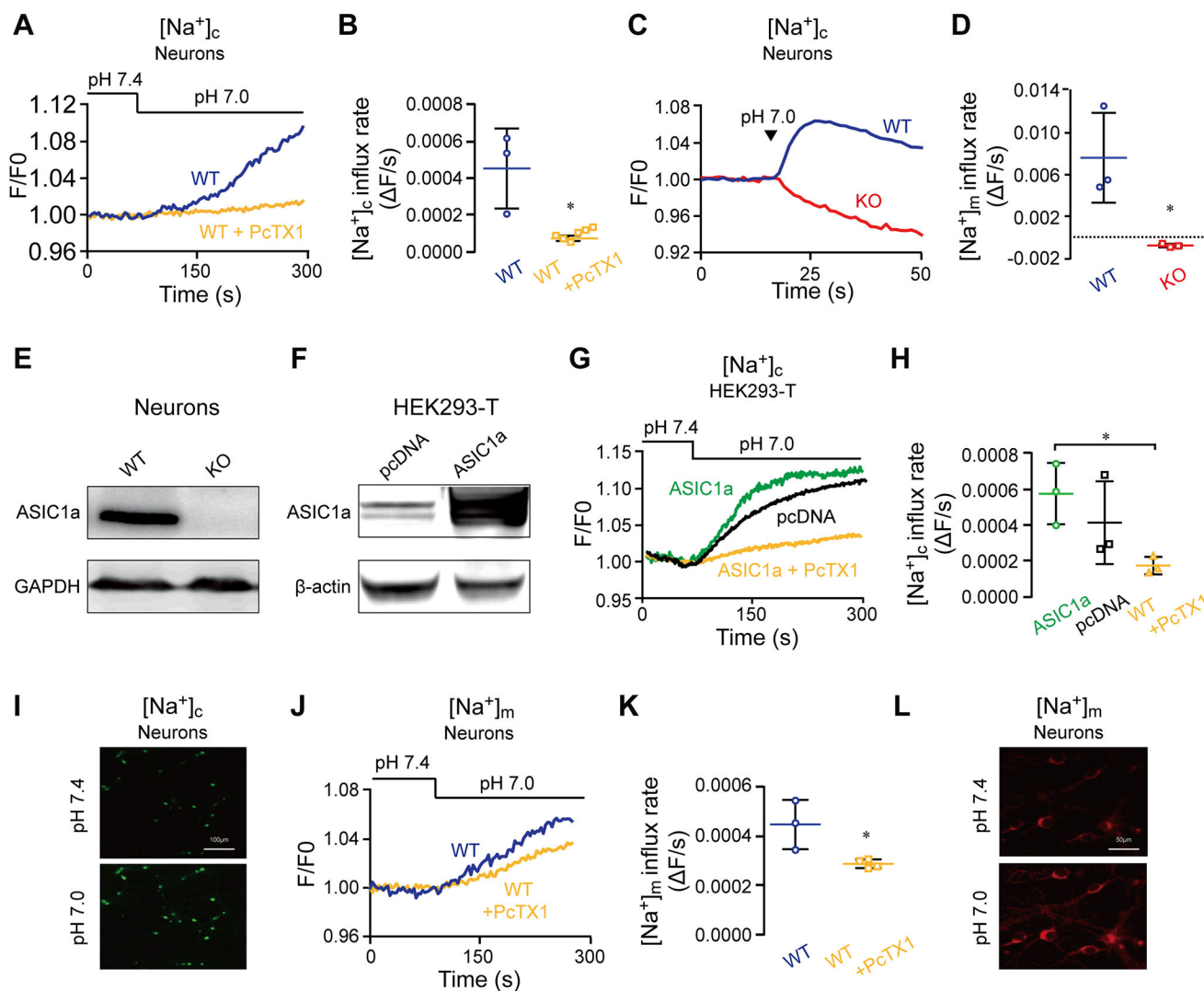


Figure 1. Activation of ASIC1a at pH 7.0 triggers cytosolic and mitochondrial Na^+ signals
 (A) Representative fluorescence traces of cytosolic Na^+ concentration ($[Na^+]_c$) changes monitored in WT primary cultured cortical neurons (DIV 10-15) without and with pretreatment of the selective ASIC1a inhibitor PcTX1 (20 nM, 120 s). Neurons were loaded with Asante NaTRIUM Green-2 (1 μ M) and initially superfused with Ringer's solution at pH 7.4. Then, the superfusion was switched to Ringer's solution of pH 7.0 as indicated.
 (B) Quantification of $[Na^+]_c$ change rates measured as in (A) for WT neurons untreated (n=3) and treated with PcTX1 (n=6).
 (C) Immunoblot analysis of ASIC1a in WT and ASIC1a KO neurons. GAPDH was used as a loading control, representative of n = 3 independent experiments.
 (D) Representative fluorescence traces of $[Na^+]_c$ changes in WT and ASIC1a KO neurons loaded with Asante NaTRIUM Green in response to pH 7.0 Ringer's solution applied through direct puffing.
 (E) Quantification of rates of $[Na^+]_c$ changes during the early phases as in (D) for WT (n=3) and ASIC1a KO (n=3) neurons.

(F) Immunoblot analysis of ASIC1a in pcDNA and ASIC1a-transfected HEK293-T cells. Actin was used as a loading control, representative of n=3 independent experiments. Note, HEK293-T cells endogenously express ASIC1a (Gunthorpe, Smith et al. 2001).

(G) Representative $[Na^+]_c$ changes in response to superfusion of the pH 7.0 solution in HEK293-T cells transfected with the empty vector and overexpressing ASIC1a without and with PcTX1 pretreatment as in (A).

(H) Quantification of rates of $[Na^+]_c$ changes as in (E) for pcDNA-transfected (n=3), ASIC1a overexpressing HEK 293-T cells untreated (n=3) and treated (n=3) with PcTX1.

(I) Representative images (x10) of neurons that were loaded with Asante NaTRIUM Green-2 before and after pH change in the presence of Na^+ . The scale bars represent 100 μm .

(J) Representative fluorescence traces for mitochondrial Na^+ concentration ($[Na^+]_m$) changes in response to superfusion of the pH 7.0 solution in WT neurons loaded with CoroNa Red (1 μM) untreated and pretreated with PcTX1.

(K) Quantification of rates of $[Na^+]_m$ increases as in (I) for WT neurons untreated (n=3) and treated with PcTX1 (n = 4).

(L) Representative images of neurons (x20) that were loaded with CoroNa Red before and after pH shift in the presence of Na^+ . The scale bars represent 50 μm .

All bar graph data represent mean \pm SEM, with n representing the number of independent cell cultures. *p < 0.05, *** p < 0.001.

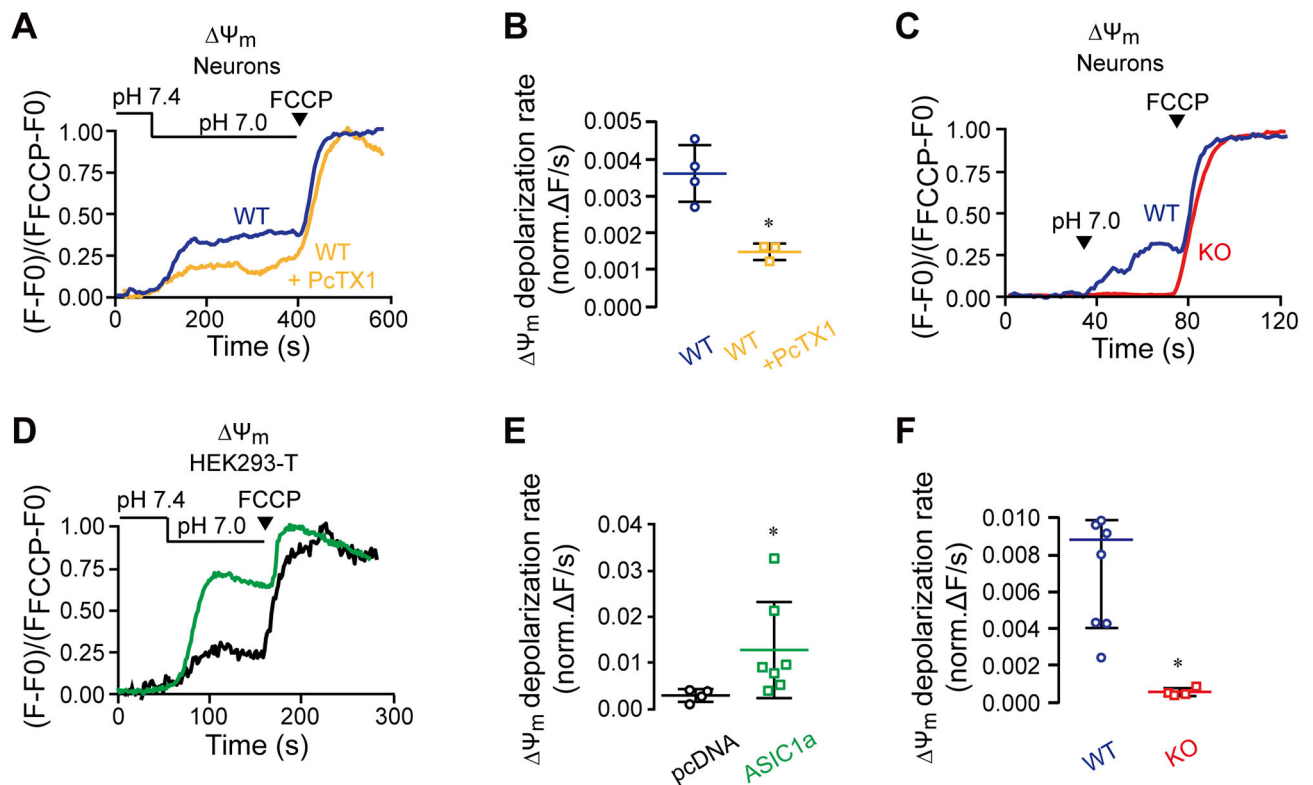


Figure 2. Physiological pH shift from 7.4 to 7.0 triggers an ASIC1a-dependent mitochondrial depolarization

Neurons were loaded with Rhodamine 123 (1.26 μM) and changes in mitochondrial membrane potential (Ψ_m) evoked by extracellular pH change from 7.4 to 7.0 were monitored using the same paradigms as described in Figure 1. FCCP (1 μM) was applied at the end of each experiment for signal calibration.

(A) Representative traces of pH-dependent changes in Ψ_m of untreated and PcTX1-pretreated WT neurons induced through superfusion.

(B) Quantification of Ψ_m depolarization rates measured as in (A) for untreated (n=4) and PcTX1-pretreated (n=3) WT neurons.

(C) Representative traces of pH-dependent changes of Ψ_m of WT and ASIC1a KO neurons induced by puffing.

(D) Quantification of Ψ_m rates determined as in (C) for WT (n=7) and ASIC1a KO (n=4) neurons.

(E) Representative traces of pH-dependent changes in Ψ_m induced through superfusion of HEK293-T cells that overexpressed ASIC1a or were transfected with the empty vector (pcDNA).

(F) Quantification of Ψ_m depolarization rates as measured in (E) for ASIC1a overexpressed (n=7) and pcDNA-transfected (n=4) HEK293-T cells.

All bar graphs show mean \pm SEM, with n representing the number of independent cell cultures. * $p < 0.05$.

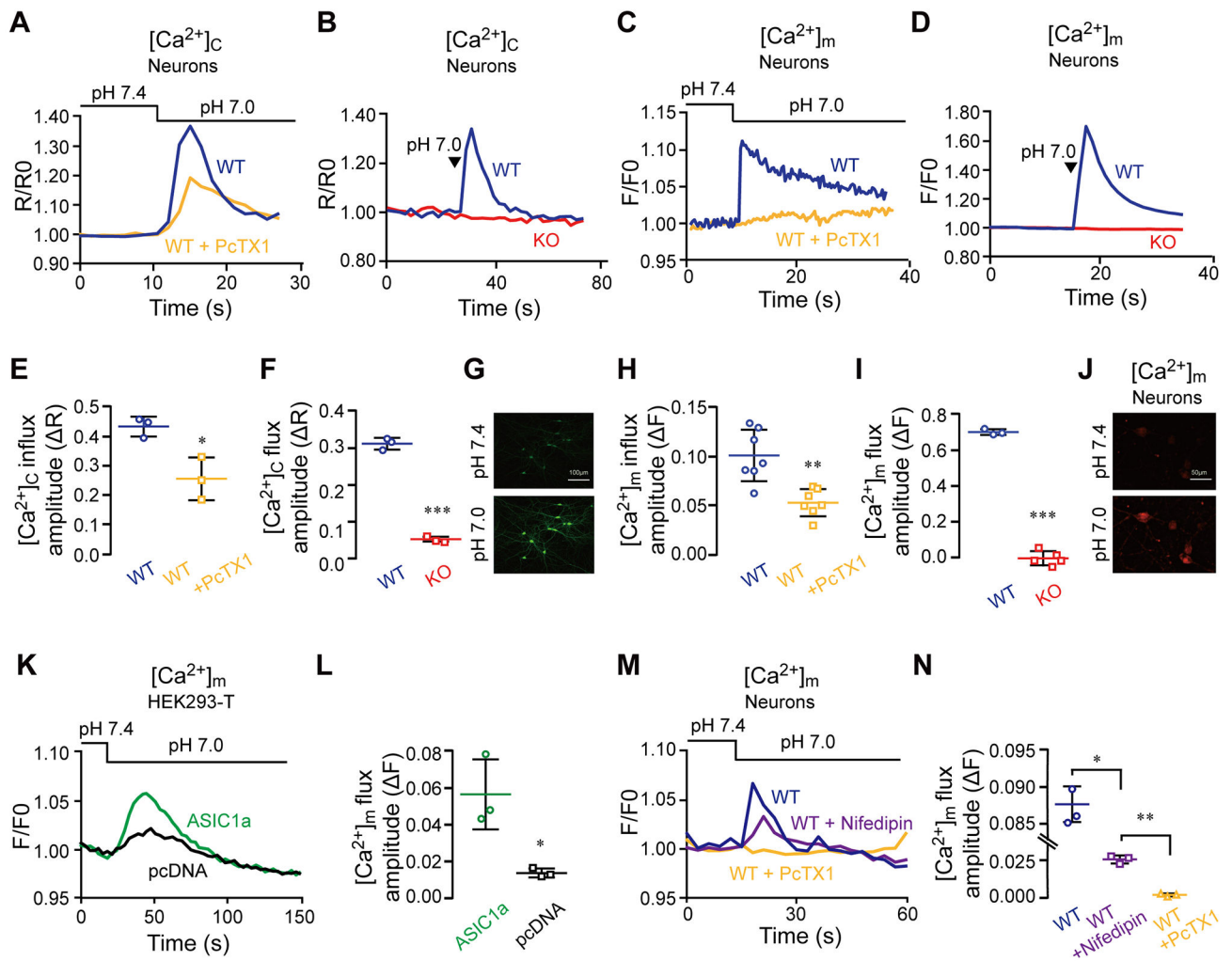


Figure 3. Physiological pH shift from 7.4 to 7.0 triggers a cytosolic Ca^{2+} response that is propagated to mitochondria

(A) Representative fluorescence ratio traces of pH-dependent cytosolic Ca^{2+} concentration ($[Ca^{2+}]_c$) changes monitored in untreated and PcTX1-pretreated WT neurons. Neurons were loaded with Fura-2-AM (1 μM) and pH change was carried out through superfusion.

(B) Quantification of $[Ca^{2+}]_c$ increase as measured in (A) for untreated (n=3) and PcTX1-pretreated (n=3) neurons.

(C) Representative fluorescence ratio traces of $[Ca^{2+}]_c$ changes induced by puffing with the pH 7.0 solution in WT and ASIC1a KO neurons loaded with Fura-2-AM.

(D) Quantification of $[Ca^{2+}]_c$ increase as determined in (C) for WT (n=3) and ASIC1a KO (n=3) neurons.

(E) Representative images of neurons (x10) that were loaded with Fura-2-AM before and after pH shift in the presence of Ca^{2+} . The scale bars represent 100 μm .

(F) Representative pH-dependent mitochondrial Ca^{2+} concentration ($[Ca^{2+}]_m$) changes induced by superfusion and monitored by fluorescence in Rhod-2 AM (1 μM) loaded WT neurons untreated and pretreated with PcTX1.

(G) Quantification of $[Ca^{2+}]_m$ changes as measured in (E) for untreated (n=7) and PcTX1-pretreated (n=7) neurons.

(H) Representative fluorescence traces of $[Ca^{2+}]_m$ changes induced by puffing the pH 7.0 solution in WT and ASIC1a KO neurons.

(I) Quantification of $[Ca^{2+}]_m$ changes determined as in (G) for WT (n=3) and ASIC1a KO (n=4) neurons.

(J) Representative images of neurons (x20) that were loaded with Rhod-2 AM before and after pH shift in the presence of Ca^{2+} . The scale bars represent 50 μ m.

(K) Representative fluorescence traces of pH-dependent $[Ca^{2+}]_m$ changes induced through superfusion in HEK293-T cells that overexpressed ASIC1a or were transfected with the empty vector (pcDNA).

(L) Quantification $[Ca^{2+}]_m$ changes determined as in (I) for HEK293-T cells that overexpressed ASIC1a (n=3) and were transfected with pcDNA vector (n=3).

(M) Representative pH-dependent mitochondrial Ca^{2+} concentration ($[Ca^{2+}]_m$) changes induced by superfusion and monitored by fluorescence in Rhod-2AM (1 μ M) loaded WT neurons pretreated with Nifedipin and PcTX1 separately.

(N) Quantification of $[Ca^{2+}]_m$ changes as measured in (K) for untreated (n=3), Nifedipin (n=3) and PcTX1-pretreated (n=3) neurons

All bar graph data represent mean \pm SEM, with n representing the number of independent cell cultures. *p < 0.05, **p < 0.01, ***p < 0.001

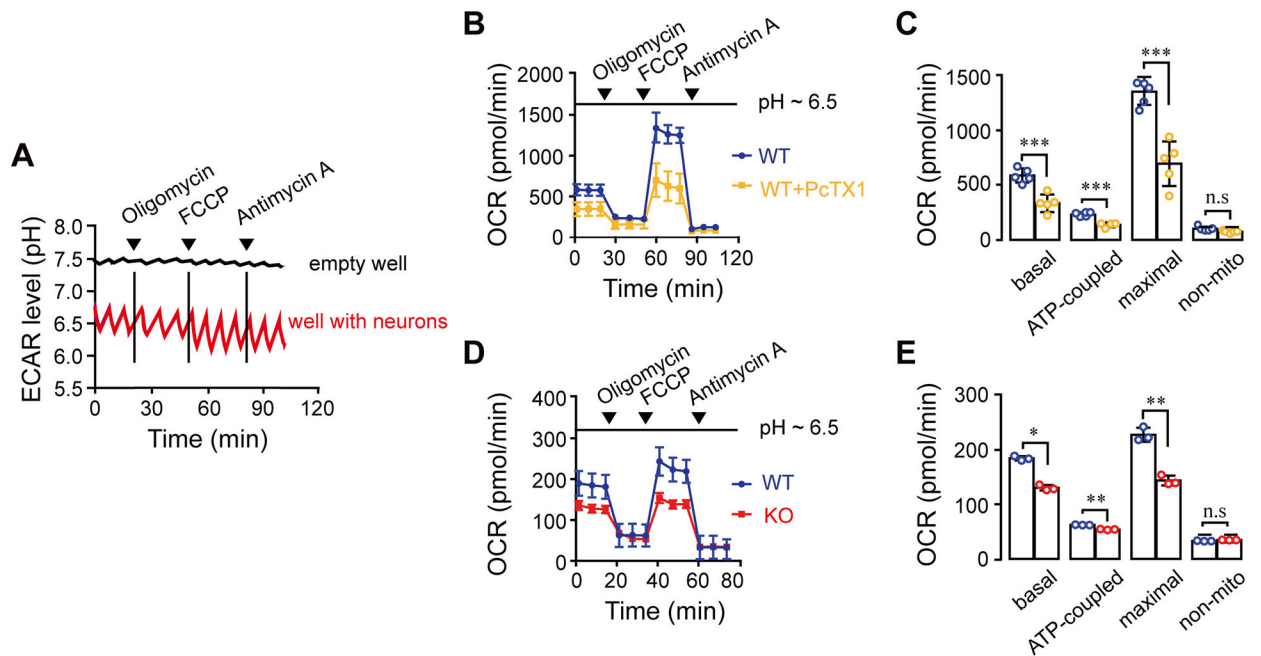


Figure 4. Physiological pH shift from 7.4 to 7.0 triggers an ASIC1a-dependent change in neuronal mitochondrial metabolic activity.

Seahorse analyses (see Materials and Methods) were used to monitor basal, maximal and ATP-coupled respiration at pH ~6.5, after addition of Oligomycin (Oligo. 1 μ M), FCCP (1 μ M) + sodium pyruvate (5 mM) (FCCP) and antimycin A (4 μ M) as indicated by the arrowheads. The low pH_e environment (pH~6.5) was induced by evoked glycolysis in medium that contained low glucose and culturing without CO_2 .

(A) Extracellular acidification rate (ECAR) levels showing the exact pH levels of the extracellular medium during 120 minutes of the experiment.

(B) Representative Oxygen Consumption Rate (OCR) traces \pm SEM measured in WT neurons with or without PcTX1 treatment.

(C) Quantification of basal, maximal, ATP-coupled and non-mitochondrial respiration as measured in (A) for untreated (n=4-5) and PcTx1-pretreated (n=4-5) WT neurons.

(D) Representative traces of OCR \pm SEM of WT and ASIC1a KO neurons.

(E) Quantification of OCR parameters as determined in (D) for WT (n=3) ASIC1 KO (n=3) neurons.

All bar graph data represent mean \pm SEM, with n representing the number of independent cell cultures, ns non-significant, * $p < 0.05$, ** $p < 0.01$, *** $p < 0.001$

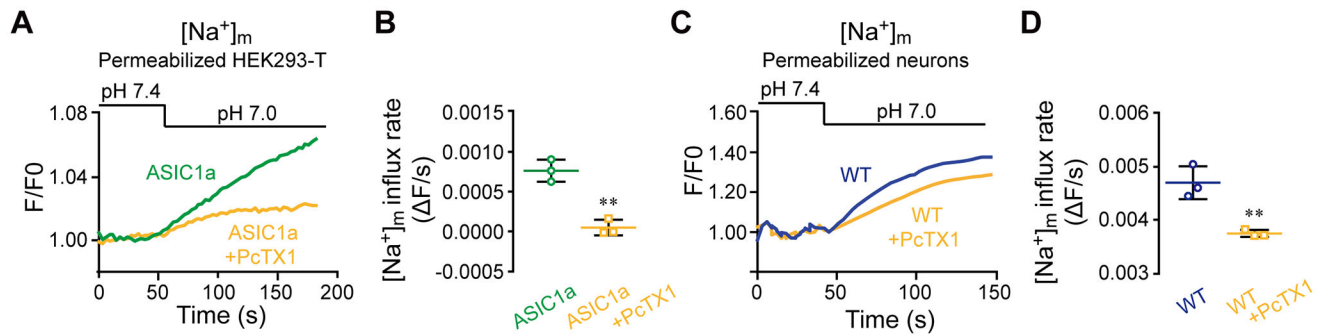


Figure 5. Mitochondrial ASIC1a plays a role in mitochondrial Na^+ signaling

(A) Representative $[Na^+]_m$ fluorescence traces in digitonin-permeabilized HEK293-T cells overexpressing ASIC1a (See Materials and Methods). Cells were loaded with CoroNa Red (1 μ M) and then untreated or treated with PcTX1 before the pH 7.0 solution was applied through superfusion.

(B) Quantification of the rate of $[Na^+]_m$ increase measured in (A) for cells untreated (n=3) and treated (n=3) with PcTX1.

(C) Representative fluorescence traces of $[Na^+]_m$ changes in response to superfusion of the pH 7.0 solution of untreated and PcTX1 pre-treated digitonin-permeabilized WT neurons.

(D) Quantification of the rate of $[Na^+]_m$ increase determined in (C) for WT neurons untreated (n = 3) and pretreated (n=3) with PcTX1.

All bar graph data represent mean \pm SEM, with n representing the number of independent cell cultures, ns non-significant **p < 0.01.

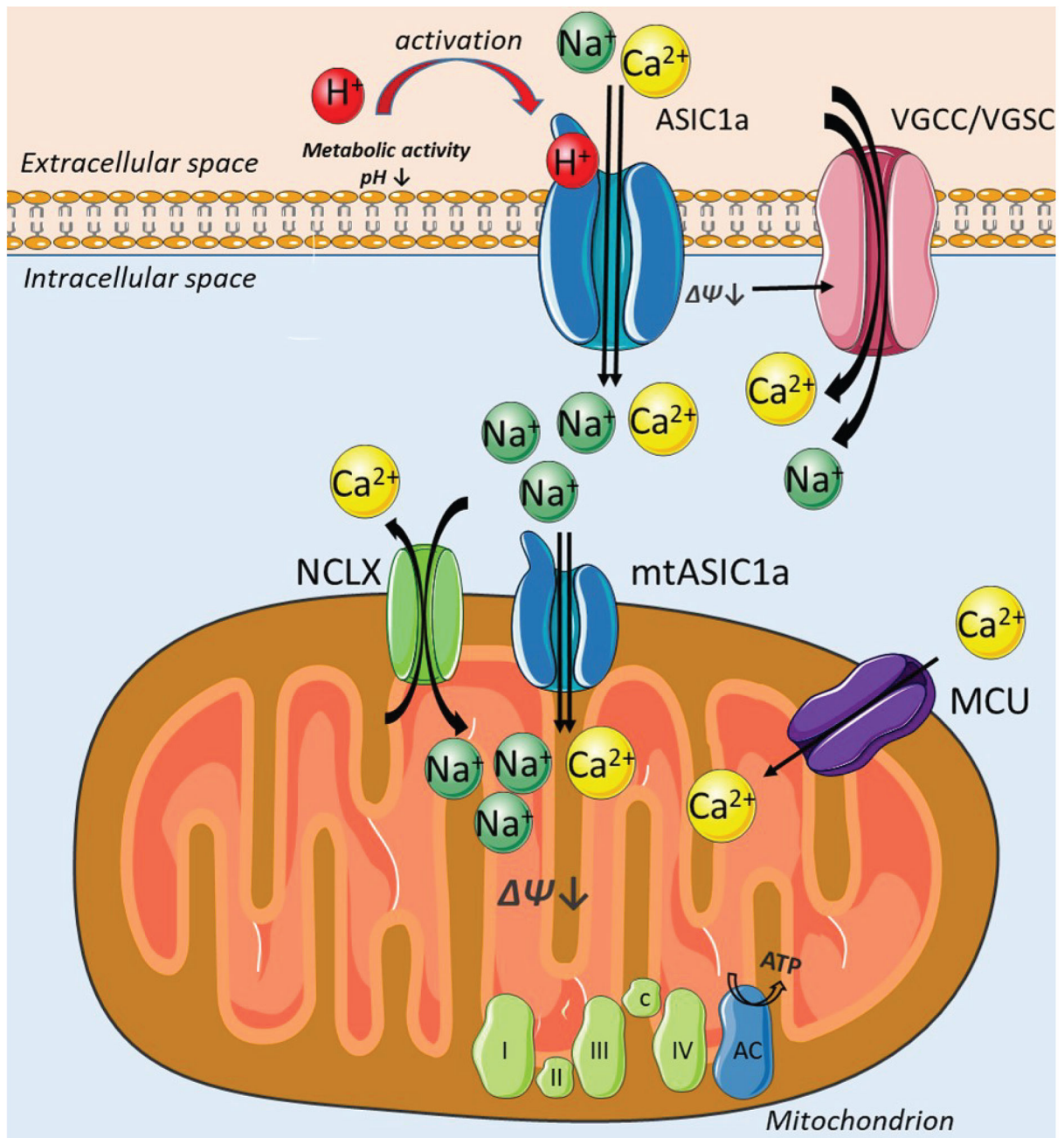


Figure 6. ASIC1a is a metabolic sensor that communicates with mitochondria to affect mitochondrial respiration.

Metabolic activity of neurons triggers mild extracellular acidification that activates plasmalemmal ASIC1a channels. Na⁺ and Ca²⁺ flow into the cytosol via ASIC1a and VGSC/VGCC and then in and out the mitochondria via MCU, NCLX and mtASIC1a. The depolarization of mitochondrial membrane and mitochondrial [Ca²⁺] rise via MCU and mtASIC1a, further affect mitochondrial respiratory chain by increasing the rate of mitochondrial respiration and thereby accelerating mitochondrial metabolic rate.